Published in final edited form as:
IEEE Trans Biomed Eng. 2014 July ; 61(7): 1967–1978. doi:10.1109/TBME.2014.2311071.

High Definition Transcranial Direct Current Stimulation Induces Both Acute and Persistent Changes in Broadband Cortical Synchronization: a Simultaneous tDCS-EEG Study

Abhrajeet Roy,
Department of Biomedical Engineering, University of Minnesota, Minneapolis, MN 55455, USA

Bryan Baxter, and
Department of Biomedical Engineering, University of Minnesota, Minneapolis, MN 55455, USA

Bin He [Fellow IEEE]
Department of Biomedical Engineering and Institute for Engineering in Medicine, University of Minnesota, Minneapolis, MN 55455 USA

Bin He: binhe@umn.edu

Abstract

The goal of this study was to develop methods for simultaneously acquiring electrophysiological data during high definition transcranial direct current stimulation (tDCS) using high resolution electroencephalography (EEG). Previous studies have pointed to the after effects of tDCS on both motor and cognitive performance, and there appears to be potential for using tDCS in a variety of clinical applications. However, little is known about the real-time effects of tDCS on rhythmic cortical activity in humans due to the technical challenges of simultaneously obtaining electrophysiological data during ongoing stimulation. Furthermore, the mechanisms of action of tDCS in humans are not well understood. We have conducted a simultaneous tDCS-EEG study in a group of healthy human subjects. Significant acute and persistent changes in spontaneous neural activity and event related synchronization (ERS) were observed during and after the application of high definition tDCS over the left sensorimotor cortex. Both anodal and cathodal stimulation resulted in acute global changes in broadband cortical activity which were significantly different than the changes observed in response to sham stimulation. For the group of 8 subjects studied, broadband individual changes in spontaneous activity during stimulation were apparent both locally and globally. In addition, we found that high definition tDCS of the left sensorimotor cortex can induce significant ipsilateral and contralateral changes in event related desynchronization (ERD) and ERS during motor imagination following the end of the stimulation period. Overall, our results demonstrate the feasibility of acquiring high resolution EEG during high definition tDCS and provide evidence that tDCS in humans directly modulates rhythmic cortical synchronization during and after its administration.

Correspondence to: Bin He, binhe@umn.edu.

Index Terms

neuromodulation; transcranial direct current stimulation; tDCS; electroencephalography; EEG; event related desynchronization; event related synchronization

I. INTRODUCTION

ELECTRICAL stimulation of the human brain has long been of interest to the scientific and medical communities. In particular, transcranial direct current stimulation (tDCS) has emerged as an effective method for noninvasively modulating human brain activity in recent years. Although neural stimulation using direct current has been investigated in animal studies as early as 1956 [1], the application of tDCS in humans was only first reported in 2000 [2]. In this early study, the investigators reported that applying small amounts of electrical current across the scalp surface was able to induce changes in cortical excitability in a group of healthy human subjects, based on post-stimulation assessments of motor evoked potential values elicited by transcranial magnetic stimulation (TMS) [2]. Importantly, anodal stimulation was found to be excitatory while cathodal stimulation was generally inhibitory. Since the initial investigation of tDCS in humans many groups have attempted to further delineate its physiological mechanisms of action. It has been suggested that the primary effects of tDCS are due to its ability to change the resting membrane potentials of pyramidal neurons in layer 5 cortex orthogonal to the scalp surface [3]–[5]. In addition, tDCS is able to induce long lasting after effects on cortical plasticity through modification of N-methyl-D-aspartate (NMDA) receptor efficiency and modification of synaptic plasticity across cortical networks [6, 7].

Behavioral studies have since revealed potential therapeutic applications of tDCS for a wide variety of disorders, including Parkinson's, stroke, depression, schizophrenia, and addiction [3, 4, 8, 9]. EEG recordings following tDCS stimulation periods have revealed changes in resting state oscillatory neural activity, functional connectivity, and event related activity during cognitive tasks. There is also evidence that tDCS of the motor cortex is able to induce changes in event related desynchronization/synchronization (ERD/ERS) during motor imagery tasks following the stimulation period [10]–[12]. These ERD/ERS signals represent time-locked changes in the synchronized firing of large populations of pyramidal neurons during the imagination of movements and often show deficits in conditions such as stroke, paralysis and other movement disorders. Thus, further optimization of tDCS methods could significantly improve clinical outcomes for motor rehabilitation, which utilizes ERD/ERS biomarkers. Furthermore, given the widespread use of such sensorimotor cortical rhythms as control signals for EEG-based brain computer interfaces (BCIs), the potential of tDCS for aiding in BCI training through the modulation of motor imagery ERD/ERS should be further explored.

Although initial reports of modulating cortical activity using tDCS are promising, very few studies have investigated *in vivo* changes in local and global brain electrical activity during the actual administration of tDCS in humans [13]–[16]. Thus, previous studies have not been able to adequately address the immediate effects of tDCS on cortical synchronization and relate them to the subsequent after effects, but instead have focused on the after effects. For

these reasons, there is a need to better understand the mechanisms and effects of tDCS in real-time in order to cater treatment protocols in a patient-specific manner, especially considering the potential future applications of tDCS for both fundamental neuroscience and clinical research.

To date, the majority of tDCS studies have utilized large, saline soaked sponge electrodes for stimulation, ranging between 25 and 35 cm^2 in surface area [9]. In this traditional configuration, one electrode is used as an anode and the other as a cathode. The use of large sponge electrodes makes it especially difficult to acquire simultaneous EEG data during stimulation as they directly obstruct the signal for EEG channels overlaying the stimulation electrodes [17]. These large electrodes are also ill-suited for focal targeting of tDCS due to the broad spatial distribution of the electric field induced during stimulation. In contrast to traditional saline soaked sponge electrodes, several studies have investigated the use of high definition stimulation electrodes for tDCS [18]–[22]. These electrodes are approximately the same size as a standard EEG electrode and allow for significantly increased current density during the application of tDCS [23]. For this reason high definition tDCS systems may be far more useful than traditional methods of tDCS for combination with EEG recording methods. High definition tDCS also offers increased spatial specificity of stimulation, which could lead to more effective targeting of cortical regions.

The aim of this study was to investigate the feasibility of recording high resolution EEG during high definition tDCS of the sensorimotor cortex. We hypothesized that tDCS would result in localized, polarity specific changes in oscillatory EEG rhythms due to subthreshold changes in neuronal resting potentials underlying the stimulation region. We further hypothesized that the effects of tDCS on cortical excitability would persist following the end of the stimulation period, as indicated by changes in motor imagination event related desynchronization/synchronization (ERD/ERS) in sensorimotor cortex. In this way we were able to link the acute effects of tDCS with its persistent after effects on synchronous neural activity.

II. MATERIALS & METHODS

A. Subjects

This study was conducted according to a protocol approved by the IRB of the University of Minnesota. Eight healthy human subjects participated in the study (range: 21–34 years old {mean: 25, standard deviation: 5.24}, 5 females). All subjects were high school graduates with some level of college education. No subjects had any history of neurological or psychological disorders. In addition, subjects had no history of substance abuse, brain lesions or metal implants. Each subject participated in three different experimental sessions: anodal, cathodal and sham stimulation. Experimental sessions were separated by a period of at least one week. Given the relatively long period of time between experimental sessions, we assumed no carry-over effects of tDCS from one session to the next. Subjects were informed of all aspects of the experiment including the possibility of minor adverse effects related to tDCS, such as transient sensations of itching, burning and prickling on the scalp, and all subjects gave informed consent at the beginning of each session. All subjects were naïve to tDCS and the aims of the study. Each subject initially came in for two experimental

sessions (anodal and sham stimulation) to assess tDCS tolerability and feasibility of the overall procedure. The order of these first two stimulation sessions was randomized by computer. After the initial sessions and establishing subject tolerability of tDCS, subjects were asked to participate in a third session during which cathodal stimulation was administered. A cognitive assessment test (mini mental states examination) was performed on each subject at the beginning and end of each experimental session to ensure cognitive normality following tDCS. Additionally, subject perception of the tDCS was assessed for each stimulation condition.

B. Simultaneous tDCS-EEG protocol

High definition tDCS was applied using a 4x1 ring electrode configuration in all experiments. For the anodal stimulation condition, one stimulation electrode was used as the anode while the other four electrodes were collectively used as the cathode. In contrast, for the cathodal stimulation condition, one stimulation electrode was used as the cathode while the other four were collectively used as the anode. In each case, the primary electrode was placed between the C3 and CP3 electrode locations on a 64 channel EEG cap (BrainProducts, GMBH, Germany) while the remaining four electrodes of opposite polarity were placed in the cap in a radial fashion (radius = 4.5 cm) around the central stimulation electrode (Fig. 1). DC current was generated using a 1x1 DC stimulator (Soterix Medical, New York City) and then split into the 5 high density Ag/AgCl sintered ring electrodes (Stens Corporation, San Rafael, CA) using a 4x1 high definition adaptor (Soterix Medical, New York City). The sham stimulation condition consisted of the same positioning of the 5 stimulation electrodes, however current was only applied at the very beginning and very end of the usual stimulation period. In this way subjects experienced the same sensations related to the ramping up and down of the DC in the sham condition as in the real stimulation conditions. A current intensity of 1.0 mA was applied for a total duration of 10 minutes over the left sensorimotor cortex during real stimulation sessions.

In each experimental session the tDCS block was approximately 20 minutes long, with EEG being recorded continuously before, during and after the stimulation, including ramping up and down periods (Fig. 2). Subjects were comfortably seated in an office chair facing an LCD computer monitor, where visual stimuli/cues were presented throughout the course of the experiment. Eyes open resting EEG was acquired using a 5000 Hz sampling frequency and a 64 channel MR compatible cap and amplifier system (BrainProducts, GMBH, Germany) while the subject fixated on a central fixation cross on the computer monitor. After three minutes, the tDCS was turned on and ramped up to 1.0 mA (ramping times varied due to differences in scalp impedances across different days). Following the ramping period, the tDCS was held at a constant current of 1.0 mA for ten minutes, while the subject continued fixation. After the tDCS period, the current was ramped down and resting EEG was recorded for an additional three minutes.

C. Motor imagination task

Subjects were also instructed to engage in a motor imagination task before and after each stimulation period in order to evaluate the after effects of each tDCS configuration on motor imagery ERD/ERS in bilateral sensorimotor cortex (Fig. 2). Each subject engaged in three

blocks of the motor imagery task both before and after tDCS. Within each motor imagery block the subject was presented with 20 trials during which they were instructed to imagine continuously clenching either their right or left hand. Each trial type was presented in an alternating fashion, starting with the presentation of a cue (GET READY) for 2 seconds, followed by the trial event (RIGHT or LEFT) for 5 seconds, during which subjects continuously imagined movement of the target hand. Each trial ended with a 3 second rest period (REST), resulting in a total time of 10 seconds for each trial. Subjects rested for approximately one minute between motor imagery blocks. EEG was continuously recorded during all motor imagery blocks and saved for offline analysis.

D. EEG data analysis

All EEG data were processed in MATLAB (The Mathworks, Inc., Natick, MA, USA) and SPSS (IBM, Armonk, NY, USA). Resting state EEG data collected during tDCS were first preprocessed by downsampling to 250 Hz and bandpass filtering between 2–50 Hz. Lower frequencies between 0–2 Hz were omitted during analysis due to the presence of large tDCS related drift artifacts under 2 Hz. In order to optimize the detection and removal of artifacts related to ongoing tDCS using independent component analysis (ICA), tDCS voltage ramping up and down epochs were first zeroed out due to the presence of very large artifacts during these periods. Additional noisy epochs were also zeroed out before concatenation of the remaining good epochs for the entire tDCS-EEG scan. Consistently noisy channels were also omitted from the analysis, resulting in 57 good channels for each subject. ICA was then utilized to identify and remove additional eye-blink, muscle and tDCS-related artifacts. tDCS-related artifacts were identified as high amplitude, random fluctuations in broadband EEG activity localized in electrodes directly adjacent to the tDCS stimulation electrodes and showed similar characteristics in both the phantom and human experiments. Low frequency random oscillations were particularly characteristic of the tDCS artifacts. Additional low frequency tDCS-related artifacts related to voltage changes driven by the DC stimulator were also identified by ICA for removal in the human experiments.

Following preprocessing, time-frequency analysis was used to determine real-time changes in cortical activity induced by tDCS during each experimental session. For each channel, a spectrogram was calculated for the 20 minute resting tDCS-EEG session. Percent changes in individual band powers during the stimulation and post-stimulation blocks were calculated with respect to the pre-stimulation baseline (30 second period before the ramping up of the tDCS) for all anode, cathode and sham sessions. Next, for each frequency band a 3-way (time-block{stimulation, post-stimulation}; condition{anode, cathode, sham}; channel{all good channels}) repeated measures ANOVA analysis was carried out to assess variances in band power changes across the three experimental configurations. In addition, Mauchly's test of sphericity was evaluated for each frequency band to assess variability across subject responses. A Greenhouse-Geisser correction was applied to all significant ANOVA effects based on the corresponding epsilon value calculated for the frequency band of interest. For frequency bands with a significant 3-way (time-block*condition*channel) interaction we followed up the 3-way ANOVA analysis with a 2-way (condition*channel) repeated measures ANOVA for each level of the time-block factor (stimulation, post-stimulation) to delineate the overall global effects of tDCS, based on the main effect of 'condition'. The

results of these ANOVAs were also corrected for non-sphericity as before. Post-hoc multiple comparisons tests (alpha = 0.05, Bonferroni corrected) were subsequently carried out to determine statistically significant differences in global responses to the three different tDCS conditions for the stimulation and post-stimulation time-blocks.

Event related time-spectral analysis was utilized for assessment of changes in motor imagery related ERD/ERS following each stimulation configuration. Motor imagery EEG data were preprocessed similar to the resting EEG data, being downsampled to 250 Hz and bandpass filtered between 2–50 Hz. All motor imagery trials for each experimental session were epoched and spectrograms were calculated for channels C3, CP3, C4 and CP4 for the right and left imagery conditions respectively. These channels were chosen for evaluation a priori as it is well established that they show robust changes in synchronization across multiple frequency bands during left and right motor imagery across subjects. Thus, we hypothesized that the real stimulation conditions would result in significantly different ERD/ERS changes in these channels compared to changes following sham stimulation due to tDCS-related effects on cortical synchronization. Bad imagery trials were automatically rejected based on six different statistical factors of the signal power in each channel: maximum, mean, median, standard deviation, skewness and kurtosis. For each band, ERD and ERS were calculated and averaged across trials by subtracting the average band power during the five second motor imagery period from the average band power during the one second baseline period preceding the GET READY cue. Positive percent change values indicated ERS while negative values indicated ERD. Overall changes in ERD/ERS due to tDCS were calculated by subtracting the average ERD/ERS values for motor imagery trials before the stimulation block from the average ERD/RES values for motor imagery trials after the stimulation block for each channel and stimulation condition. These values were then pooled to obtain average percent change values for two regions of interest (ROIs): left sensorimotor cortex (channels C3, CP3) and right sensorimotor cortex (channels C4, CP4). For each imagery direction and frequency band, planned contrasts were evaluated between the real stimulation (anode, cathode) ERD/ERS changes and the sham ERD/ERS changes for each ROI. Since two non-orthogonal contrasts were evaluated for each ROI at each level combination we utilized a Bonferroni corrected alpha of 0.025 (0.05/2) for all comparisons. The family-wise mean square error for each planned contrast was obtained from a corresponding one-way (condition{anode, cathode, sham}) repeated measures ANOVA for the given ROI, imagery direction and frequency band. A critical t value of 2.0796 (two-tailed, df = 21, alpha = 0.025) was used to determine significant t-statistics calculated for all contrasts. Planned contrasts were evaluated independently for each combination of ROI and imagery direction for several main reasons. First, a greater degree of noise was expected in the left sensorimotor cortex (SMC) channels (C3, CP3) due to their proximity to the tDCS electrodes throughout each experimental session. Second, a greater change in ERD/ERS was anticipated for the right imagery condition given that the left SMC was targeted using tDCS. Finally, individuals often have a “preferred” or “dominant” motor imagery direction which results in a large variance in bilateral ERD/ERS responses for each imagery direction at the group level. Given that the goal of this part of the study was to delineate potentially subtle, localized group level effects of tDCS on motor imagery using a relatively small sample size,

statistical analyses combining the already variable elements of ROI and imagery direction was not appropriate.

E. Phantom experiments

The simultaneous tDCS-EEG protocol was first run using a phantom head model (garden melon) in order to make preliminary assessments regarding the characteristics of the tDCS related artifacts and the overall feasibility of the experimental procedure. It was particularly important to optimize methods for removal of the tDCS related artifacts during acute stimulation in order to reliably delineate the actual neural responses to ongoing DC stimulation. Conductive EEG gel was smeared across the entirety of the phantom prior to placement of the EEG cap. Individual EEG channel and tDCS electrode impedances were then lowered using additional conductive gel. As in the human experiments, 1.0 mA tDCS was then applied for 10 minutes using the anode, cathode and sham configurations, respectively. Following experimentation, changes in the global field power (GFP) were calculated throughout the course of each session to determine if tDCS artifacts induced any changes in overall signal power during different periods of tDCS. Time-frequency analysis was also performed to determine specific noise effects of tDCS in different frequency bands in the absence of neural activity. ICA was then utilized to identify the spatiotemporal characteristics of artifacts induced by the 4x1 high definition tDCS for each experimental configuration. These noise components were removed from the continuous data and time-frequency analysis was again used to assess ongoing changes in band power during tDCS in the clean data. The phantom experiments allowed us to more confidently utilize ICA for tDCS-related artifact removal in the subsequent human experiments.

III. RESULTS

A. Phantom experiments and removal of tDCS-related EEG artifacts

One of the major goals of this study was to evaluate the feasibility and technical challenges of simultaneous tDCS-EEG. To this extent, all EEG data were manually assessed throughout the various stages of preprocessing in order to ensure data quality. We performed a series of phantom experiments to first evaluate the feasibility of our tDCS-EEG protocol and delineate the characteristics of artifactual EEG components arising from ongoing DC stimulation using the 4x1 high definition ring electrode configuration. We observed a number of EEG artifacts related to the tDCS in these initial phantom experiments. The most prominent artifacts were observed during the ramping up and down of the stimulation current, during which large voltage fluctuations appeared not only in channels adjacent to the five high density tDCS electrodes but also globally across both sides of the EEG cap. These ramping up and down periods were zeroed out prior to ICA in order to focus on analysis of the EEG during the “ramped up” period when the tDCS was held constant at 1.0 mA. However, prior to zeroing out these periods the average signal power and its standard deviation were calculated for each channel to determine electrodes significantly affected during the tDCS procedure in each experimental session. Identification of these electrodes allowed for more careful evaluation of artifactual ICs related to tDCS in subsequent preprocessing stages, given the variations in head size, shape and conductivity at the subject level. Additional large low frequency drift artifacts (<2 Hz) due to tDCS were also observed

in EEG electrodes adjacent to tDCS electrodes throughout the entire tDCS period. For this reason we chose to ultimately filter the data between 2–50 Hz as this minimized the prevalence of the more prominent low frequency drift artifacts prior to ICA for removal of residual drift artifacts.

No significant changes in GFP were observed during the phantom tDCS-EEG session between the pre-stimulation baseline, stimulation period and post-stimulation baseline before ICA-based noise removal. Thus, time-frequency analysis was utilized to investigate frequency specific changes in phantom EEG activity due to ongoing tDCS during the ramped up period. We found that the tDCS device induced localized, broadband EEG noise only during active stimulation (no noise was observed simply due to the tDCS-EEG experimental setup). The ongoing tDCS strongly contaminated the raw EEG signal in channels C3 and CP3 (adjacent to the central tDCS stimulation electrodes) as well as additional EEG channels adjacent to the four surround tDCS electrodes, particularly in low frequency bands (Type I artifacts). Using ICA, we were able to effectively identify and remove these channel artifacts due to ongoing tDCS, which appeared to be a result of tDCS currents drifting across the phantom surface and effecting subsequent electrical potential readings in EEG channels in close proximity (Fig. 3). Broadband noise observed in channels directly adjacent to the main stimulation electrode (C3, CP3) was effectively removed with this ICA procedure. Following cleaning of the phantom data using ICA we still observed some global fluctuations in individual frequency band powers relative to baseline during and after the stimulation period. However these changes were extremely small in magnitude and not spatially correlated with the locations of the tDCS electrodes. Such fluctuations were similarly observed using the sham stimulation configuration on the phantom model, further suggesting that they are due to random noise and not the tDCS itself. Importantly, band power values for the phantom experiment were several orders of magnitude smaller than those observed in human experiments, making these ongoing, residual fluctuations in band power negligible during later analysis of the human data.

tDCS related artifacts observed during human experiments were generally identical to those observed during the phantom experiments, allowing for consistent manual identification and removal of bad ICs across subjects before further data analysis (Fig. 3). Interestingly, additional channel artifacts due to the tDCS stimulator maintaining a constant current were also observed in nearly all human experiments (Type II artifacts). This additional artifact appeared to be due to a regularized low frequency voltage fluctuation induced by the tDCS device itself, in order to maintain a constant stimulation current (1.0 mA). Furthermore, these artifacts often increased steadily in signal strength over the course of the 10 minutes of stimulation, potentially indicating a gradual increase in EEG channel impedance and subsequent increase in the voltage gradient required to maintain the constant current. The signal profile of this artifact type was also identical to that of the artifacts related to the tDCS stimulator ramping up and down the voltage, further reiterating the need for its removal prior to assessing changes in actual neural activity related to tDCS.

B. Subject-specific responses to ongoing tDCS

Following development of our preprocessing procedures we investigated subject-specific changes in spontaneous cortical activity during and after tDCS. First, the GFP of the continuous EEG data was averaged across three different time windows for each experimental session: 30 seconds pre-ramp-up baseline, 10 minutes stimulation period, 30 seconds post-ramp-down baseline. No significant changes in the average GFP relative to baseline was observed during or after stimulation for any of the three experimental conditions, as in the phantom experiments. Given the absence of overall changes in global EEG power due to tDCS, we utilized time-frequency analysis to delineate subject-specific changes in neural activity in different frequency bands. This allowed us to look at changes in spontaneous cortical synchronization relative to the pre-stimulation baseline during and after both anodal and cathodal tDCS. Subjects showed large local and global increases in cortical synchrony relative to the position of the tDCS electrodes during anodal stimulation (Fig. 4, 5). Local effects in channel CP3 were most apparent, although the breadth of frequency bands affected varied across subjects. Additionally, most subjects only showed large increases in activity during anodal stimulation versus after. Cathodal stimulation similarly resulted in acute, local increases in activity with respect to the stimulation ROI, in addition to decreases in broadband frontal activity in 5 of the 8 subjects (Fig. 5). Interestingly, large variations in spontaneous cortical activity were also seen during the sham condition, although significant, focal changes in band power relative to the stimulation ROI were not consistently seen as in the real-tDCS conditions.

Subject perception of stimulation was also assessed in each experiment in order to ensure comfort and safety of the overall experimental protocol. No significant adverse effects to stimulation were reported by any of the subjects and we found no decreases in cognitive indices in any subjects following stimulation based on our mini-mental states examination. The stimulation sensation was most consistently described as a burning/prickling sensation on the scalp directly underlying the central tDCS electrode. Sensation was most pronounced during the ramping up and down periods, though minor sensations were transiently felt during the ramped up stimulation period in some cases.

C. Group level responses to ongoing tDCS

Group level responses to high definition tDCS and sham stimulation of the left sensorimotor cortex were investigated to determine the generalized acute effects of stimulation. Overall percent changes in band power relative to the pre-stimulation baseline were evaluated for the stimulation and post-simulation blocks for each experimental condition (anode, cathode, sham) across all frequency bands of interest. A 3-way repeated measures ANOVA analysis was subsequently carried out for each frequency band. Separate Mauchly's tests of sphericity revealed non-sphericity for all frequency bands of interest (Table 1). Greenhouse-Geisser epsilon values were also calculated for each frequency band in order to adjust the results of the corresponding 3-way ANOVAs. Following these corrections, a significant 3-way (time-block*condition*channel) interaction effect was found for the delta, theta and alpha bands (Table 2). No significant 3-way interaction was found for the beta band, although significant 2-way interactions of condition*channel ($F(53,374)=1.616$, $p=0.006$)

and time-block*channel ($F(26,187)=3.584$, $p<0.001$) were apparent. No significant main level or interaction effects were found for the gamma band.

In order to further interpret the significant 3-way interactions found for the delta, theta and alpha bands, we followed up each 3-way ANOVA with a 2-way (condition{anode, cathode, sham}, channel{all good channels}) repeated measures ANOVA for each level of the time-block factor (stimulation, post-stimulation). 2-way ANOVAs were corrected for non-sphericity as before. A significant main effect of 'condition' was found for the delta, theta and alpha bands for the stimulation block. For the post-stimulation block a significant main effect of 'condition' was only found for the delta and alpha bands (Table 3). For all 2-way ANOVAs showing a significant main effect of 'condition', we carried out post-hoc multiple comparisons tests (alpha = 0.05, Bonferroni corrected) to determine significant stimulation and post-stimulation differences in the global effects of tDCS between the three experimental conditions (Fig. 6). Cathodal stimulation resulted in a significantly smaller delta band response (+22%) during the stimulation block compared to both the anode (+64%) and sham (+55%) conditions. Similarly, cathodal stimulation showed a smaller post-stimulation effect in the delta band (+44%) compared to the anode (99%) and sham (+109%) conditions. For the theta band, anodal stimulation resulted in a significantly greater response (+53%) during the stimulation block compared to both the cathode (+19%) and sham (+31%) conditions, with the cathodal response also being significantly less than the sham response. The alpha band response to anodal stimulation was significantly higher during the stimulation block (+93%) compared to both the cathode (+43%) and sham (+70%) conditions, with the cathodal response also being significantly less than the sham response. However, the sham condition had a significantly greater post-stimulation effect on alpha power (+88%) compared to both the anode (+49%) and cathode (+55%) conditions.

D. Group level changes in motor imagery ERD/ERS following tDCS

In addition to investigating the acute effects of tDCS on spontaneous cortical activity we also evaluated changes in event related synchronization in the sensorimotor cortex following the stimulation period for each experimental condition. In order to achieve this, we investigated changes in ERD/ERS during left and right motor imagination of the hand before and after the simultaneous tDCS-EEG resting state period. Trials related to left and right motor imagery were extracted using a ten second window centered on the respective onset of the visual cue for imagination (−4:6 seconds) for channels C3, CP3, C4 and CP4. The relative change in ERD/ERS during motor imagery before and after the stimulation period was calculated for each channel across frequency bands. For each subject, percent change values for each frequency band and imagery direction were averaged across channels C3 and CP3 to obtain a single percent change value for the left sensorimotor cortex (SMC) while values across channels C4 and CP4 were averaged to obtain a single percent change value for the right SMC.

Planned comparisons between the anode and sham conditions and cathode and sham conditions were evaluated for both ROIs (left and right SMC) for each combination of imagery direction and frequency band. A Bonferroni corrected alpha value of 0.025 (0.05/2) was used for each planned contrast to account for the two non-orthogonal comparisons that

were evaluated for each ROI. Significant differences for the right motor imagery condition were found for the theta, beta and gamma bands (Fig. 7). Theta band synchronization in right SMC significantly decreased following sham stimulation (−12%) compared to anodal stimulation (+13%) during right motor imagery. Beta band synchronization in left SMC significantly decreased following sham stimulation (−15%) compared to anodal stimulation (+12%) during right motor imagery. Beta band synchronization in right SMC also significantly decreased following sham stimulation (−11%) compared to anodal stimulation (+13%) during right motor imagery. Finally, gamma band synchronization in left SMC significantly decreased following sham stimulation (−7%) compared to cathodal stimulation (+8%) during right motor imagery. No significant changes in ERD/ERS were found for the left motor imagery condition for either region of interest.

IV. DISCUSSION

The present study evaluated both the real-time and post-stimulation effects of high definition tDCS over the left sensorimotor cortex on spontaneous cortical activity and event related cortical synchronization in a group of healthy human subjects. In particular, we demonstrated the feasibility of simultaneously recording EEG during tDCS for assessment of acute group level responses to stimulation. To our knowledge, this is the first study to directly investigate the *in vivo* acute effects of high definition 4x1 tDCS on spontaneous cortical rhythms in humans using high resolution EEG obtained during active stimulation and relate them to the persistent after effects of tDCS on motor imagery ERD/ERS. Previous studies using simultaneous tDCS-EEG methods have been very limited in scope, generally only recording EEG from a single electrode during stimulation [15], [24], [25]. Overall, we found significant global differences in spontaneous cortical activity across multiple frequency bands using both anodal and cathodal stimulation configurations with respect to the sham stimulation condition. Furthermore, we observed significant changes in bilateral motor imagery ERD/ERS across multiple frequency bands following tDCS.

Our results reiterate early findings of animal studies of transcranial DC polarization which reported polarity specific changes in spontaneous neural firing during stimulation [1], [26]–[29]. Importantly, these early animal studies found that changes in cortical excitability were not frequency specific and persisted following the end of the stimulation period for up to several hours if DC was applied for an appropriately long duration [26], [27]. Early studies of tDCS in humans added support to the notion that tDCS could in fact induce long lasting changes in cortical excitability and functional connectivity, despite the relatively small amount of electrical energy being transferred to the brain [2, 6, 7]. Furthermore, the primary effects of tDCS have been hypothesized to be due to tonic depolarization/hyperpolarization of large populations of pyramidal cells oriented orthogonal to the cortical surface [3], [30], resulting in increased or decreased spontaneous firing activity, respectively. Our results support this assertion, given that we found significant polarity specific changes in spontaneous cortical activity during tDCS using EEG, a direct measure of electrical activity being produced by the synchronization of pyramidal cells. Specifically, we found differing global effects of tDCS on resting EEG activity depending on the polarity of stimulation. Anodal stimulation generally resulted in significantly greater global synchronization across frequency bands when compared to the cathodal and sham conditions. In contrast, cathodal

stimulation resulted in significantly lower global synchronization across frequency bands when compared to the anodal and sham conditions. These results are well in line with previous studies that have shown that anodal stimulation is generally excitatory while cathodal stimulation is generally inhibitory [2].

We further investigated the effects of different tDCS configurations on motor imagery ERD/ERS across different frequency bands following the stimulation period. It is well established that planning or imagining hand movements leads to a desynchronization (ERD) in the alpha (8–13 Hz) and beta (13–30 Hz) bands in the region of the motor cortex contralateral to the imagined hand while concurrently increasing synchronization (ERS) in these frequency bands in the ipsilateral motor cortex [31]–[33]. This sensorimotor EEG response in the alpha and beta bands during motor imagery is well established for use in brain-computer interfaces for motor rehabilitation [34]–[36]. However, subjects substantially vary in their ability to elicit consistent motor imagery responses in the EEG, often resulting in a significant bottleneck towards mastery of the BCI. tDCS of the motor cortex has previously been shown to improve motor learning, suggesting it could potentially be used to improve subject mastery of sensorimotor-based BCIs [37]. Our results demonstrate that tDCS can significantly modulate theta, beta and gamma band synchronization during motor imagination ERD/ERS. Anodal stimulation of the left sensorimotor cortex significantly increased contralateral ERS in the theta band during right motor imagery. Anodal stimulation also significantly reduced ipsilateral beta band ERD while significantly increasing contralateral beta band ERS during right motor imagery. Collectively, these results suggest that anodal stimulation of one hemisphere can increase bilateral cortical synchronization in the beta band, possibly due in part to intrahemispheric connections. In contrast, cathodal stimulation of the left sensorimotor cortex significantly increased ipsilateral gamma band ERS during right motor imagery. These results further demonstrate the polarity-dependent effects of tDCS. Future work should aim to make a preliminary assessment of subject-specific ERD/ERS responses during motor imagery and tailor the subsequent tDCS protocol based on this initial assessment. Our findings make it difficult to assess the potential of using tDCS specifically for training subjects to use sensorimotor rhythm-based BCIs. However, such effects on cortical excitability could be of use for rehabilitation of neural disorders which exhibit significantly reduced or altered network synchronization in various frequency bands, such as stroke, paralysis, schizophrenia and depression [4], [8], [38].

Our results could help to explain the large variation in reports of the effects of tDCS on cortical activity in the literature and add to the growing body of work utilizing functional neuroimaging methods for investigating the effects of tDCS. We observed global and local changes in both spontaneous and event related EEG activity during and after tDCS, respectively. Since we found that tDCS does not affect cortical rhythms in a strictly frequency specific manner, its subsequent effects on cognitive and motor processing could be due to modulation of a broad range of oscillatory neural activity involved in such tasks. Many other groups have similarly reported changes in cortical synchrony across frequency bands following traditional tDCS using saline soaked sponge electrodes. In general these studies assessed electrophysiological activity using EEG before and after a period of stimulation of the region of interest [17], [39]–[42], or EEG recordings interleaved between

short periods of stimulation [43], [44]. tDCS over the left motor cortex has previously been shown to induce changes in motor imagination ERD/ERS in a polarity dependent manner, although reports of the polarity specific effects vary [11], [45], [46]. These results emphasize that motor imagery is a complex cognitive process and its origins are not entirely understood. However, similar to our results, reduced ERD following anodal stimulation and increased ERD following cathodal stimulation has been reported [45]. Thus, tonic cortical depolarization/hyperpolarization using tDCS could modulate ERD/ERS through effects on both cortical excitability and subcortical network activity. For instance, increasing excitability could increase spontaneous neural activity and noise, resulting in reduced event related desynchronization, while the opposite effects could arise from decreasing spontaneous excitability. Anodal tDCS of left M1 has also been shown to induce broadband changes in both ipsilateral and contralateral EEG functional connectivity during motor imagery following stimulation [41]. Such changes in global functional connectivity could help explain the global effects of tDCS on broadband synchronization we observed here. Modulation of oscillatory EEG activity in specific frequency bands has also been achieved following frequency specific tDCS (oscillatory tDCS) and tACS (transcranial alternating current stimulation) [43], [47]–[50]. Elevated band power in the delta, theta and alpha bands were reported in such studies [16].

Functional magnetic resonance imaging has also been used to investigate the real-time effects of tDCS on hemodynamic activity [51]–[55]. Although the BOLD signal is an indirect measure of neural activity, it is well established that the BOLD signal changes relative to large changes in synchronized neural activity which may be directly recorded using EEG [56]–[59]. MRI studies have revealed that both anodal and cathodal stimulation of the motor cortex can increase regional cerebral blood flow and the BOLD signal [52], [54], [60]. In addition, widespread ipsilateral and contralateral changes in resting state network functional connectivity can be observed following M1 tDCS, particularly within motor, premotor and supplementary motor areas [12], [61]. Our EEG results are well in line with these findings, given that we observed acute and persistent global changes in neural synchronization for both the anode and cathode conditions. Magnetoencephalography (MEG) may also be a method for assessing the real-time electrophysiological effects of tDCS. Soekadar et al. recently established the feasibility of collecting MEG recordings during tDCS with large electrodes (6x4 cm) in a small group of healthy subjects [13]. They reported broadband MEG artifacts related to tDCS during the stimulation period which were similar to those we observed in the EEG. However, this study did not include a sham condition and did not report any significant group level effects of tDCS. Furthermore, the use of large, flat electrodes likely resulted in substantially different current flows over the scalp than those induced by our high definition tDCS configurations.

This study establishes the feasibility of simultaneous tDCS-EEG in healthy human subjects using high resolution recording and stimulation electrodes. Given the promise of this technique, further work is needed to optimize the data acquisition and analyses procedures. ICA proved to be effective for identification and removal of artifacts related to ongoing tDCS. Faria et al. recently similarly evaluated the feasibility of simultaneous tDCS-EEG for the study of spike-wave discharges during slow wave sleep in human epilepsy, although they did not report any specific results regarding changes in cortical synchronization related

to tDCS [14]. ICA was successfully utilized offline in order to remove tDCS artifacts caused by the DC stimulator, as we demonstrated in our methods as well. Future studies should utilize a more automated procedure for ICA based detection and removal of tDCS-related EEG artifacts. Although we were able to remove the majority of the tDCS artifacts using linear (ICA) methods, there is the possibility that some residual artifacts remain in the signal due to broadband Brownian noise induced near the stimulation electrodes. However, the effects of this noise seem negligible at the group level given the differing global effects of anodal and cathodal stimulation we report here and the lack of such noise in the ICA-cleaned phantom data. Regardless, artifact removal using a combined linear and non-linear approach may further improve EEG resolution in evaluating the acute local effects of tDCS. The development of algorithms for real-time removal of tDCS-related EEG artifacts would also be of significant value for future applications of tDCS in BCI training, sleep studies and studies of epilepsy [62]. Our study did not investigate real-time changes in event related potentials (ERPs) induced during tDCS but instead observed changes in event related synchronous activity following the tDCS period. Future work with simultaneous tDCS-EEG will need to investigate changes in both evoked and spontaneous brain activity during stimulation. This study did not investigate changes in EEG activity during the ramping up and down of the tDCS current; due to the presence of large artifacts these sections were zeroed out prior to ICA removal of residual tDCS-related artifacts. Developing methods for removing these ramping artifacts would allow for the investigation of tDCS-related brain activity changes with full time resolution. Finally, neither stimulation configuration used in this study was truly unipolar. In reality, each configuration was a combination of anodal and cathodal stimulation points which likely resulted in complex local current flows and contributed to the wide range of subject-specific changes seen in response to the tDCS. Future studies of tDCS-EEG will need to integrate computational modeling, anatomical MRI scans and stereoscopic targeting to optimize tDCS treatment protocols for individual subjects, similar to recent TMS, deep brain stimulation and transcranial ultrasound stimulation studies [63]–[68].

V. CONCLUSION

Our results have significant implications for applications of tDCS in both fundamental neuroscience and clinical research. This is, to our knowledge, the first study to directly investigate the acute effects of 4x1 high definition tDCS in humans using high resolution EEG and relate them to the subsequent after effects of stimulation. Importantly, we found significant global EEG changes in spontaneous cortical synchronization across the delta, theta and alpha bands in response to high definition tDCS. Persistent effects of tDCS on theta, beta and gamma band synchronization were also apparent during motor imagination following stimulation. Both anodal and cathodal stimulation appeared to have both ipsilateral and contralateral effects on cortical activity. Collectively, these results reiterate the hypothesized mechanisms of action of tDCS in humans and add further evidence that tDCS is able to modulate wide-scale neural networks noninvasively. Further exploration using tDCS-EEG techniques could significantly advance our capability to target specific cortical regions for modulation in order to advance various clinical rehabilitation procedures and perhaps ultimately enhance cognition in healthy humans.

Acknowledgments

This work was supported in part by NSF CBET-1264782, NSF DGE-1069104, NIH R01EB006433, NIH T32EB008389, and ONR N000141110690.

The authors acknowledge faculty and students at the Biomedical Functional Imaging and Neuroengineering Laboratory and Center for Neuroengineering at the University of Minnesota for helpful comments and discussions.

References

1. Terzuolo CA, Bullock TH. Measurement of Imposed Voltage Gradient Adequate to Modulate Neuronal Firing. PNAS. Sep; 1956 42(9):687–694. [PubMed: 16589932]
2. Nitsche MA, Paulus W. Excitability changes induced in the human motor cortex by weak transcranial direct current stimulation. J Physiol. Sep; 2000 527(3):633–639. [PubMed: 10990547]
3. Johnson MD, Lim HH, Netoff TI, Connolly AT, Johnson N, Roy A, Holt A, Lim KO, Carey JR, Vitek JL, He B. Neuromodulation for brain disorders: challenges and opportunities. IEEE Trans Biomed Eng. Mar; 2013 60(3):610–624. [PubMed: 23380851]
4. Brunoni AR, Fregni F, Pagano RL. Translational research in transcranial direct current stimulation (tDCS): a systematic review of studies in animals. Rev Neurosci. 2011; 22(4):471–481. [PubMed: 21819264]
5. Rahman A, Reato D, Arlotti M, Gasca F, Datta A, Parra LC, Bikson M. Cellular effects of acute direct current stimulation: somatic and synaptic terminal effects. J Physiol (Lond). May; 2013 591(Pt 10):2563–2578. [PubMed: 23478132]
6. Nitsche MA, Liebetanz D, Lang N, Antal A, Tergau F, Paulus W. Safety criteria for transcranial direct current stimulation (tDCS) in humans. Clinical Neurophysiology. Nov; 2003 114(11):2220–2222. [PubMed: 14580622]
7. Nitsche M, Fricke K, Henschke U, Schlitterlau A, Liebetanz D, Lang N, Henning S, Terga F, Paulus W. Pharmacological modulation of cortical excitability shifts induced by transcranial direct current stimulation in humans. Journal of Physiology. Nov; 2003 533(1):293–301. [PubMed: 12949224]
8. Berlim MT, Van den Eynde F, Daskalakis ZJ. Clinical utility of transcranial direct current stimulation (tDCS) for treating major depression: A systematic review and meta-analysis of randomized, double-blind and sham-controlled trials. Journal of Psychiatric Research.
9. Nitsche MA, Cohen LG, Wassermann EM, Priori A, Lang N, Antal A, Paulus W, Hummel F, Boggio PS, Fregni F, Pascual-Leone A. Transcranial direct current stimulation: State of the art 2008. Brain Stimulation. Jul; 2008 1(3):206–223. [PubMed: 20633386]
10. Kasashima Y, Fujiwara T, Matsushika Y, Tsuji T, Hase K, Ushiyama J, Ushiba J, Liu M. Modulation of event-related desynchronization during motor imagery with transcranial direct current stimulation (tDCS) in patients with chronic hemiparetic stroke. Experimental Brain Research. 2012; 221(3):263–268. [PubMed: 22791228]
11. Matsumoto J, Fujiwara T, Takahashi O, Liu M, Kimura A, Ushiba J. Modulation of mu rhythm desynchronization during motor imagery by transcranial direct current stimulation. J Neuroeng Rehabil. Jun.2010 7:27. [PubMed: 20540721]
12. Peña-Gómez C, Sala-Lonch R, Junqué C, Clemente IC, Vidal D, Bargalló N, Falcón C, Valls-Solé J, Pascual-Leone Á, Bartrés-Faz D. Modulation of large-scale brain networks by transcranial direct current stimulation evidenced by resting-state functional MRI. Brain Stimulation. Jul; 2012 5(3): 252–263. [PubMed: 21962981]
13. Soekadar SR, Witkowski M, Cossio EG, Birbaumer N, Robinson SE, Cohen LG. In vivo assessment of human brain oscillations during application of transcranial electric currents. Nature Communications. Jun.2013 4
14. Faria P, Fregni F, Sebastião F, Dias AI, Leal A. Feasibility of focal transcranial DC polarization with simultaneous EEG recording: Preliminary assessment in healthy subjects and human epilepsy. Epilepsy & Behavior. Nov; 2012 25(3):417–425. [PubMed: 23123281]
15. Miniussi C, Brignani D, Pellicciari MC. Combining Transcranial Electrical Stimulation With Electroencephalography: A Multimodal Approach. Clinical EEG and Neuroscience. Apr; 2012 43(3):184–191. [PubMed: 22715493]

16. Herrmann CS, Rach S, Neuling T, Strüber D. Transcranial alternating current stimulation: a review of the underlying mechanisms and modulation of cognitive processes. Frontiers in Human Neuroscience. 2013; 7

17. Spitoni GF, Cimmino RL, Bozzacchi C, Pizzamiglio L, Di Russo F. Modulation of spontaneous alpha brain rhythms using low-intensity transcranial direct-current stimulation. Frontiers in Human Neuroscience. 2013; 7

18. Borckardt JJ, Bikson M, Frohman H, Reeves ST, Datta A, Bansal V, Madan A, Barth K, George MS. A pilot study of the tolerability and effects of high-definition transcranial direct current stimulation (HD-tDCS) on pain perception. J Pain. Feb; 2012 13(2):112–120. [PubMed: 22104190]

19. Datta A, Bansal V, Diaz J, Patel J, Reato D, Bikson M. Gyri-precise head model of transcranial direct current stimulation: Improved spatial focality using a ring electrode versus conventional rectangular pad. Brain Stimulation. Oct; 2009 2(4):201–207.e1. [PubMed: 20648973]

20. Bikson M, Rahman A, Datta A. Computational Models of Transcranial Direct Current Stimulation. Clin EEG Neurosci. Jul; 2012 43(3):176–183. [PubMed: 22956646]

21. Dmochowski JP, Datta A, Bikson M, Su Y, Parra LC. Optimized multi-electrode stimulation increases focality and intensity at target. Journal of Neural Engineering. Aug.2011 8(4):046011. [PubMed: 21659696]

22. Edwards D, Cortes M, Datta A, Minhas P, Wassermann EM, Bikson M. Physiological and modeling evidence for focal transcranial electrical brain stimulation in humans: a basis for high-definition tDCS. NeuroImage.

23. Villamar MF, Volz MS, Bikson M, Datta A, DaSilva AF, Fregni F. Technique and Considerations in the Use of 4x1 Ring High-definition Transcranial Direct Current Stimulation (HD-tDCS). Journal of Visualized Experiments. Jul.2013 (77)

24. Accornero N, Li Voti P, La Riccia M, Gregori B. Visual evoked potentials modulation during direct current cortical polarization. Experimental Brain Research. Oct; 2006 178(2):261–266. [PubMed: 17051377]

25. Schroeder M, Barr R. Quantitative analysis of the electroencephalogram during cranial electrotherapy stimulation. Clinical Neurophysiology. Nov; 2001 112(11):2075–2083. [PubMed: 11682346]

26. Bindman LJ, Lippold OCJ, Redfearn JWT. Long-lasting Changes in the Level of the Electrical Activity of the Cerebral Cortex produced by Polarizing Currents. Nature. Nov; 1962 196(4854): 584–585. [PubMed: 13968314]

27. Bindman LJ, Lippold OCJ, Redfearn JWT. The action of brief polarizing currents on the cerebral cortex of the rat (1) during current flow and (2) in the production of long-lasting after-effects. J Physiol. Aug; 1964 172(3):369–382. [PubMed: 14199369]

28. Purpura DP, McMurtry JG. Intracellular Activities and Evoked Potential Changes During Polarization of Motor Cortex. J Neurophysiol. Jan; 1965 28(1):166–185. [PubMed: 14244793]

29. Goddard GV, McIntyre DC, Leech CK. A permanent change in brain function resulting from daily electrical stimulation. Experimental Neurology. Nov; 1969 25(3):295–330. [PubMed: 4981856]

30. Stagg CJ, Nitsche MA. Physiological basis of transcranial direct current stimulation. Neuroscientist. Feb; 2011 17(1):37–53. [PubMed: 21343407]

31. Yuan H, Liu T, Szarkowski R, Rios C, Ashe J, He B. Negative covariation between task-related responses in alpha/beta-band activity and BOLD in human sensorimotor cortex: an EEG and fMRI study of motor imagery and movements. Neuroimage. Feb; 2010 49(3):2596–2606. [PubMed: 19850134]

32. Wang T, Deng J, He B. Classifying EEG-based motor imagery tasks by means of time–frequency synthesized spatial patterns. Clinical Neurophysiology. Dec; 2004 115(12):2744–2753. [PubMed: 15546783]

33. Qin L, He B. A wavelet-based time–frequency analysis approach for classification of motor imagery for brain–computer interface applications. Journal of Neural Engineering. Dec; 2005 2(4): 65–72. [PubMed: 16317229]

34. Doud AJ, Lucas JP, Pisansky MT, He B. Continuous Three-Dimensional Control of a Virtual Helicopter Using a Motor Imagery Based Brain-Computer Interface. PLoS ONE. Oct.2011 6(10):e26322. [PubMed: 22046274]
35. Royer AS, Rose ML, He B. Goal selection versus process control while learning to use a brain–computer interface. Journal of Neural Engineering. Jun.2011 8(3):036012. [PubMed: 21508492]
36. LaFleur K, Cassady K, Doud A, Shades K, Rogin E, He B. Quadcopter control in three-dimensional space using a noninvasive motor imagery-based brain–computer interface. Journal of Neural Engineering. Aug.2013 10(4)
37. Reis J, Robertson EM, Krakauer JW, Rothwell J, Marshall L, Gerloff C, Wassermann EM, Pascual-Leone A, Hummel F, Celnik PA, Classen J, Floel A, Ziemann U, Paulus W, Siebner HR, Born J, Cohen LG. Consensus: Can transcranial direct current stimulation and transcranial magnetic stimulation enhance motor learning and memory formation? Brain Stimulation. Oct; 2008 1(4):363–369.
38. Peckham PH, Kilgore KL. Challenges and Opportunities in Restoring Function After Paralysis. IEEE Transactions on Biomedical Engineering. Mar; 2013 60(3):602–609. [PubMed: 23481680]
39. Jacobson L, Ezra A, Berger U, Lavidor M. Modulating oscillatory brain activity correlates of behavioral inhibition using transcranial direct current stimulation. Clinical Neurophysiology. May; 2012 123(5):979–984. [PubMed: 21995999]
40. Keeser D, Padberg F, Reisinger E, Pogarell O, Kirsch V, Palm U, Karch S, Möller HJ, Nitsche MA, Mulert C. Prefrontal direct current stimulation modulates resting EEG and event-related potentials in healthy subjects: A standardized low resolution tomography (sLORETA) study. NeuroImage. Mar; 2011 55(2):644–657. [PubMed: 21146614]
41. Polanía R, Nitsche MA, Paulus W. Modulating functional connectivity patterns and topological functional organization of the human brain with transcranial direct current stimulation. Human Brain Mapping. 2011; 32(8):1236–1249. [PubMed: 20607750]
42. Zaehle T. Behavioral and electrophysiological effects of transcranial direct current stimulation of the parietal cortex in a visuo-spatial working memory task. Front Psychiatry. 2012; 3:56. [PubMed: 22723784]
43. Marshall L, Kirov R, Brade J, Mölle M, Born J. Transcranial Electrical Currents to Probe EEG Brain Rhythms and Memory Consolidation during Sleep in Humans. PLoS ONE. Feb.2011 6(2):e16905. [PubMed: 21340034]
44. Marshall L, Mölle M, Hallschmid M, Born J. Transcranial Direct Current Stimulation during Sleep Improves Declarative Memory. J Neurosci. Nov; 2004 24(44):9985–9992. [PubMed: 15525784]
45. Lapenta OM, Minati L, Fregni F, Boggio PS. Je pense donc je fais: transcranial direct current stimulation modulates brain oscillations associated with motor imagery and movement observation. Front Hum Neurosci. Jun.2013 7
46. Tohyama T, Fujiwara T, Matsumoto J, Honaga K, Ushiba J, Tsuji T, Hase K, Liu M. Modulation of Event-related Desynchronization duringMotor Imagery with Transcranial Direct Current Stimulationin a Patient with Severe Hemiparetic Stroke: A Case Report. The Keio Journal of Medicine. 2011; 60(4):114–118. [PubMed: 22200635]
47. Zaehle T, Rach S, Herrmann CS. Transcranial Alternating Current Stimulation Enhances Individual Alpha Activity in Human EEG. PLoS ONE. Nov.2010 5(11):e13766. [PubMed: 21072168]
48. Neuling T, Rach S, Wagner S, Wolters CH, Herrmann CS. Good vibrations: Oscillatory phase shapes perception. NeuroImage. Nov.2012 :8. [PubMed: 24179753]
49. Marshall L, Helgadóttir H, Mölle M, Born J. Boosting slow oscillations during sleep potentiates memory. Nature. Nov; 2006 444(7119):610–613. [PubMed: 17086200]
50. Reato D, Gasca F, Datta A, Bikson M, Marshall L, Parra LC. Transcranial Electrical Stimulation Accelerates Human Sleep Homeostasis. PLoS Comput Biol. Feb.2013 9(2):e1002898. [PubMed: 23459152]
51. Alon G, Roys SR, Gullapalli RP, Greenspan JD. Non-invasive electrical stimulation of the brain (ESB) modifies the resting-state network connectivity of the primary motor cortex: A proof of concept fMRI study. Brain Research. Jul.2011 1403:37–44. [PubMed: 21696709]

52. Antal A, Polania R, Schmidt-Samoa C, Dechent P, Paulus W. Transcranial direct current stimulation over the primary motor cortex during fMRI. NeuroImage. Mar; 2011 55(2):590–596. [PubMed: 21211569]
53. Antal A, Bikson M, Datta A, Lafon B, Dechent P, Parra LC, Paulus W. Imaging artifacts induced by electrical stimulation during conventional fMRI of the brain. NeuroImage.
54. Antal A, Kovács G, Chaieb L, Cziraki C, Paulus W, Greenlee MW. Cathodal stimulation of human MT+ leads to elevated fMRI signal: A tDCS-fMRI study. Restor Neurol Neurosci. Jan; 2012 30(3):255–263. [PubMed: 22475855]
55. Polanía R, Paulus W, Nitsche MA. Reorganizing the Intrinsic Functional Architecture of the Human Primary Motor Cortex during Rest with Non-Invasive Cortical Stimulation. PLoS ONE. Jan.2012 7(1):e30971. [PubMed: 22303478]
56. Liu Z, He B. fMRI-EEG integrated cortical source imaging by use of time-variant spatial constraints. Neuroimage. Feb; 2008 39(3):1198–1214. [PubMed: 18036833]
57. Liu Z, Ding L, He B. Integration of EEG/MEG with MRI and fMRI in Functional Neuroimaging. IEEE Eng Med Biol Mag. 2006; 25(4):46–53. [PubMed: 16898658]
58. He B, Liu Z. Multimodal Functional Neuroimaging: Integrating Functional MRI and EEG/MEG. IEEE Rev Biomed Eng. Nov; 2008 1(2008):23–40. [PubMed: 20634915]
59. He, Bin; Coleman, T.; Genin, GM.; Glover, G.; Hu, Xiaoping; Johnson, N.; Liu, Tianming; Makeig, S.; Sajda, P.; Ye, Kaiming. Grand Challenges in Mapping the Human Brain: NSF Workshop Report. IEEE Transactions on Biomedical Engineering. Nov; 2013 60(11):2983–2992. [PubMed: 24108705]
60. Zheng X, Alsop DC, Schlaug G. Effects of transcranial direct current stimulation (tDCS) on human regional cerebral blood flow. NeuroImage. Sep; 2011 58(1):26–33. [PubMed: 21703350]
61. Kirimoto H, Ogata K, Onishi H, Oyama M, Goto Y, Tobimatsu S. Transcranial direct current stimulation over the motor association cortex induces plastic changes in ipsilateral primary motor and somatosensory cortices. Clinical Neurophysiology. Apr; 2011 122(4):777–783. [PubMed: 21074492]
62. Chen LL, Madhavan R, Rapoport BI, Anderson WS. Real-Time Brain Oscillation Detection and Phase-Locked Stimulation Using Autoregressive Spectral Estimation and Time-Series Forward Prediction. IEEE Transactions on Biomedical Engineering. Mar; 2013 60(3):753–762. [PubMed: 21292589]
63. Zorn L, Renaud P, Bayle B, Goffin L, Lebosse C, de Mathelin M, Foucher J. Design and Evaluation of a Robotic System for Transcranial Magnetic Stimulation. IEEE Transactions on Biomedical Engineering. Mar; 2012 59(3):805–815. [PubMed: 22186930]
64. Song, Junho; Pulkkinen, A.; Huang, Yuexi; Hynynen, K. Investigation of Standing-Wave Formation in a Human Skull for a Clinical Prototype of a Large-Aperture, Transcranial MR-Guided Focused Ultrasound (MRgFUS) Phased Array: An Experimental and Simulation Study. IEEE Transactions on Biomedical Engineering. Feb; 2012 59(2):435–444. [PubMed: 22049360]
65. Gattinger N, Mossnang G, Gleich B. flexTMS-A Novel Repetitive Transcranial Magnetic Stimulation Device With Freely Programmable Stimulus Currents. IEEE Transactions on Biomedical Engineering. Jul; 2012 59(7):1962–1970. [PubMed: 22531742]
66. Schmidt C, van Rienen U. Modeling the Field Distribution in Deep Brain Stimulation: The Influence of Anisotropy of Brain Tissue. IEEE Transactions on Biomedical Engineering. Jun; 2012 59(6):1583–1592. [PubMed: 22410323]
67. Schmidt C, Grant P, Lowery M, van Rienen U. Influence of Uncertainties in the Material Properties of Brain Tissue on the Probabilistic Volume of Tissue Activated. IEEE Transactions on Biomedical Engineering. May; 2013 60(5):1378–1387. [PubMed: 23269746]
68. Zhang, Xiaotong; Yan, Dandan; Zhu, Shanan; He, Bin. Noninvasive Imaging of Head-Brain Conductivity Profiles. IEEE Engineering in Medicine and Biology Magazine. Sep; 2008 27(5):78–83. [PubMed: 18799394]

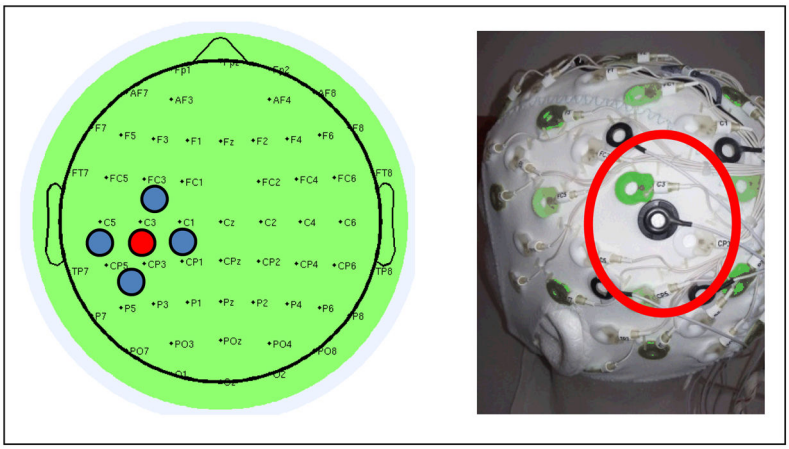

Fig. 1.

Experimental set-up for simultaneous high density tDCS and EEG. Left: Placement of tDCS ring electrodes over left sensorimotor cortex in a 4x1 configuration. For anodal stimulation, the anode was placed between EEG electrodes C3 and CP3 with the four collective cathodes oriented in a radial fashion (radius = 4.5 cm) around it. Electrode polarities were inverted during cathodal stimulation. Right: High density ring electrodes integrated into the EEG cap prior to lowering impedances using gels. The red circle indicates the target region for stimulation (left sensorimotor cortex).

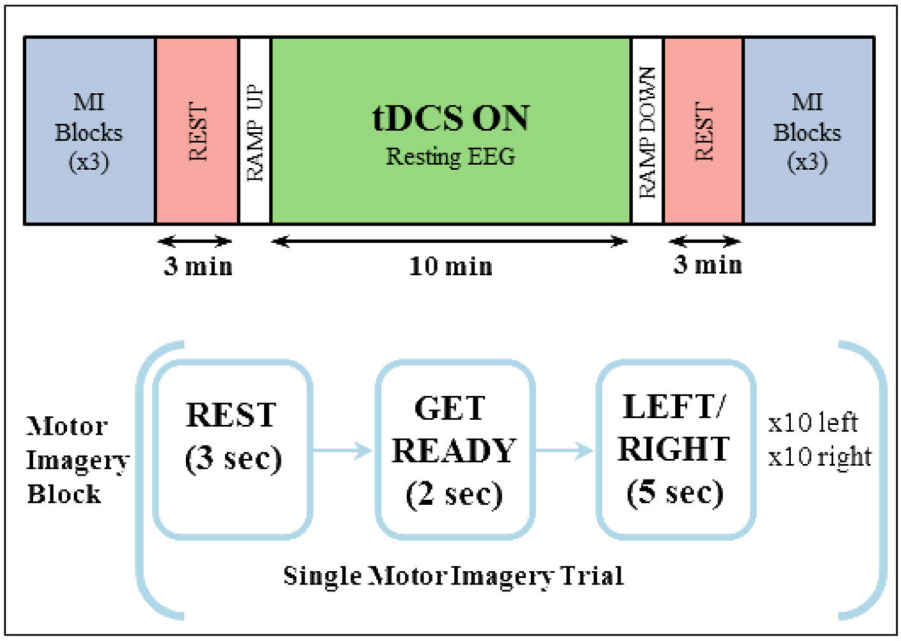

Fig. 2.

Experimental paradigm. Top: Block diagram of the experimental protocol for a single tDCS-EEG session. Subjects performed a series of motor imagery (MI) tasks before and after the stimulation block in each session. The ramping up and down periods for the tDCS block were 60 and 90 seconds for the real and sham stimulation configurations, respectively. During real stimulation, either anodal or cathodal tDCS was administered for 10 minutes using a constant current intensity of 1.0 mA. For sham sessions the stimulator only administered current during the ramp up and down blocks, with no current being administered during the 10 minutes of resting EEG. Bottom: motor imagery task description. 30 trials each of left and right hand motor imagination were performed both before and after each stimulation period. Each trial was 10 seconds long and contained a rest period, cue period and task period.

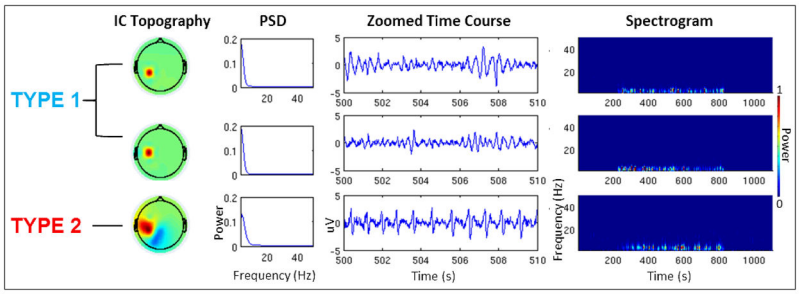

Fig. 3.

Artifactual independent components related to ongoing tDCS. Rows one (phantom-session) and two (human-session) show examples of Type I artifactual components due to random drifting of the ongoing tDCS current in EEG electrodes directly adjacent to tDCS stimulation electrodes. Row three (human-session) shows one example of a Type II artifactual component related to ongoing small shifts in voltage due to the DC stimulator maintaining a constant current of 1.0 mA. Low frequency dominated power spectral densities and spectrograms are characteristic of both artifact types.

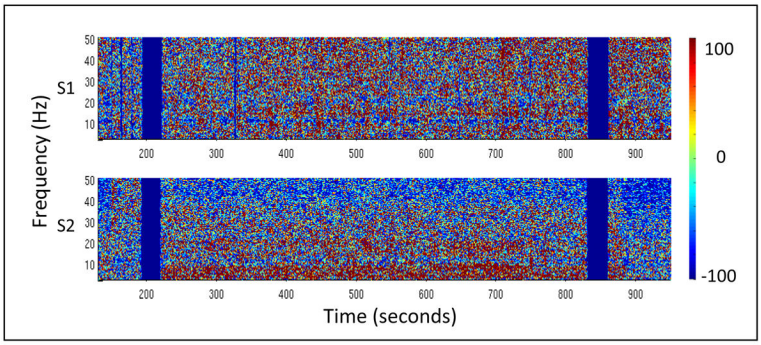

Fig. 4.

Individual subject percent changes in CP3 band power relative to baseline during anodal stimulation. Broadband increases in band power synchronization were consistently seen during tDCS across subjects. Several subjects showed sustained increases in CP3 synchronization following the end of the stimulation (S1) while other subjects showed only temporarily elevated synchronization following the end of the stimulation (S2). Blue blocks are bad epochs which were removed prior to ICA-based artifact removal.

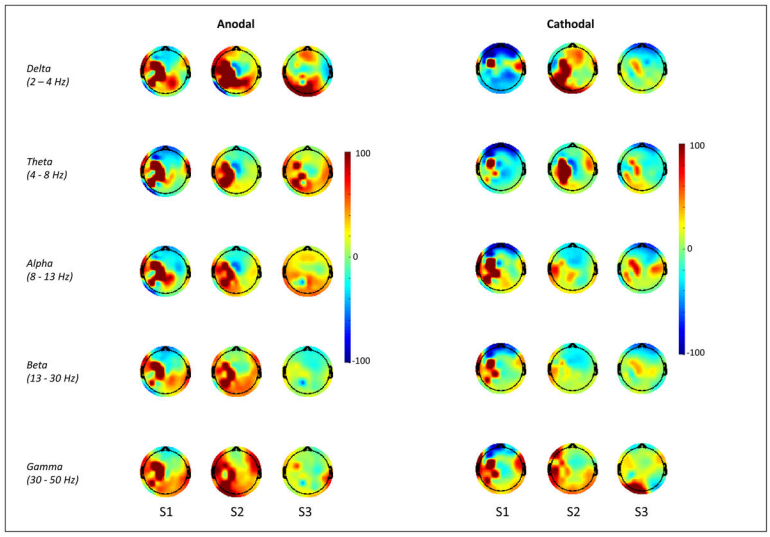

Fig. 5.

Individual subject percent changes in average band power relative to baseline during HD-tDCS using a 4x1 ring configuration. Left: Typical subject responses to anodal stimulation - broadband increases in spontaneous activity were observed across subjects, generally localized to the left sensorimotor cortex under the anode tDCS electrode. Right: Typical subject responses to cathodal stimulation – increases in activity were observed near anodal tDCS electrode positions while decreases in activity were observed in bilateral frontal regions.

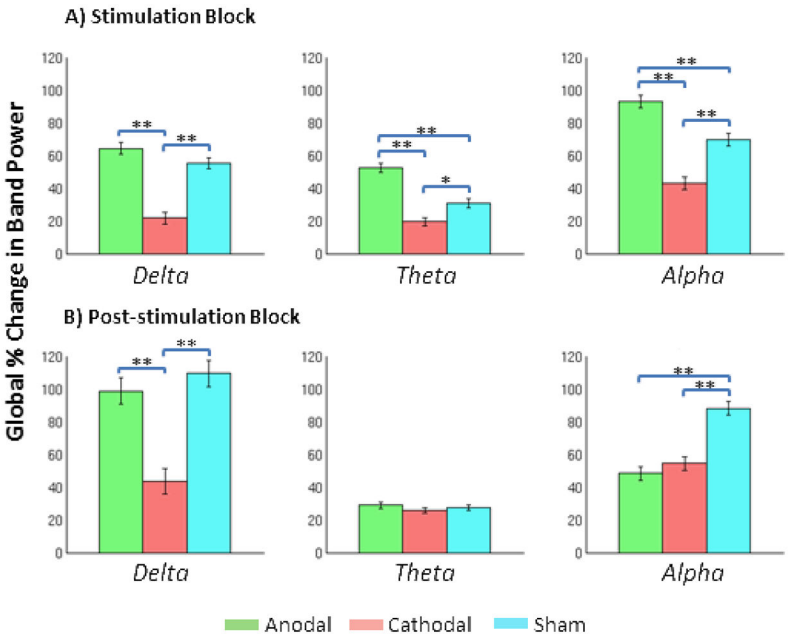

Fig. 6.

Global percent changes in band power relative to the pre-stimulation baseline for the stimulation and post-stimulation blocks. Global responses to anodal stimulation during the stimulation block were significantly higher than those observed for the sham condition for the theta and alpha bands. In contrast, global responses to cathodal stimulation during the stimulation block were significantly lower than those observed for the sham condition for the delta, theta and alpha bands. Significant differences between stimulation conditions were identified using post-hoc multiple comparisons tests for all 2-way ANOVAs of interest (*$p<0.05$, **$p<0.001$, Bonferroni corrected).

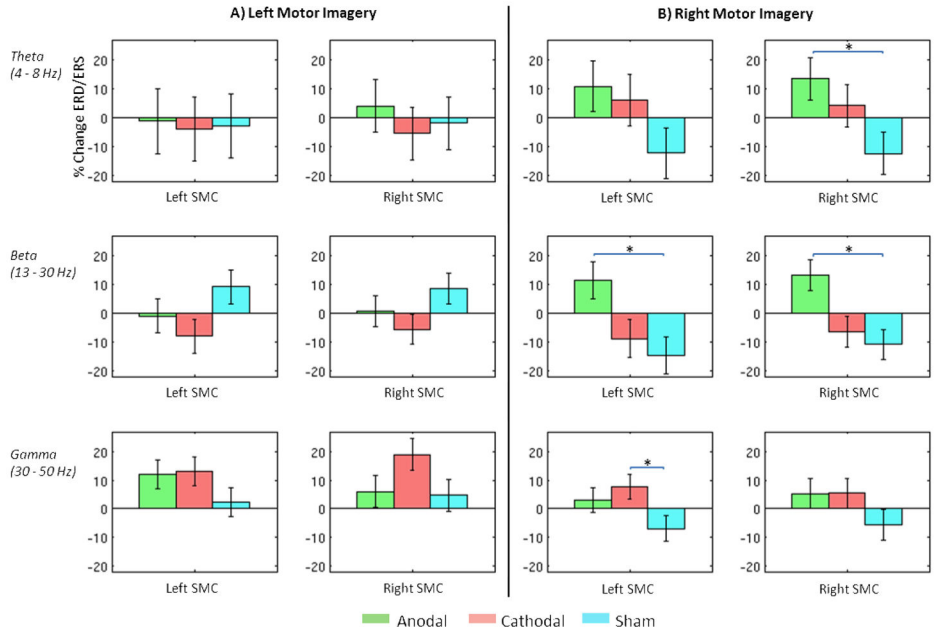

Fig. 7.

Group level percent changes in motor imagery ERD/ERS following anodal, cathodal and sham tDCS. Left two columns: overall changes in left and right sensorimotor cortex (SMC) ERD/ERS during left motor imagery for the theta, beta and gamma bands. Right two columns: overall changes in left and right SMC ERD/ERS during right motor imagery for the theta, beta and gamma bands. Two planned comparisons were evaluated for each SMC region of interest at each combination of frequency band and motor imagery direction (*$p<0.025$, Bonferroni corrected).

Table 1

Results of sphericity tests for each frequency band. Mauchly's tests of sphericity revealed non-sphericity for all frequency bands of interest. For each frequency band, the Greenhouse-Geisser epsilon value was used to adjust the results of all corresponding repeated measures ANOVA analyses (both 3- and 2-way).

Results of Mauchly's Tests of Sphericity				
Band	**Mauchly's W**	**Chi-Square (df=27)**	**p**	**Greenhouse-Geisser ε**
Delta (2–4 Hz)	0.038	1103.502	<0.001*	0.502
Theta (4–8 Hz)	0.131	687.418	<0.001*	0.592
Alpha (8–13 Hz)	0.012	1495.828	<0.001*	0.435
Beta (13–30 Hz)	0.02	1326.43	<0.001*	0.478
Gamma (30–50 Hz)	<0.001	4339.005	<0.001*	0.185

Table 2

Results of 3-way ANOVAs for each frequency band. A significant 3-way interaction was found for the delta, theta and alpha bands. No significant interactions of interest werefound for the beta and gamma bands.

3-way ANOVA Results (ε corrected)	
Band	**Time-Block*Condition*Channel**
Delta (2–4 Hz)	***F*(56,393) = 1.469, p=0.021***
Theta (4–8 Hz)	***F*(66,464) = 3.202, p<0.001***
Alpha (8–13 Hz)	***F*(48,341) = 1.566, p=0.013***
Beta (13–30 Hz)	*F*(53,374) = 1.263, p=0.114
Gamma (30–50 Hz)	*F*(20,145) = 0.919, p=0.564

Table 3

Results of 2-way ANOVAs. To determine the main effect of the stimulation condition, 2-way repeated measures ANOVA analyses were carried out for each time-block (stimulation, post-stimulation) for frequency bands which showed a significant 3-way interaction (delta, theta and alpha). A significant main level effect of condition was found for all three bands during the stimulation block, while only the delta and alpha bands showed a significant main level effect of condition for the post-stimulation block.

2-way ANOVA Results (ε corrected)		
Band	**Condition (stimulation)**	**Condition (post-stimulation)**
Delta (2–4 Hz)	***F*(1,653) = 40.379, p<0.001***	***F*(1,653) = 19.565, p<0.001***
Theta (4–8 Hz)	***F*(1,770) = 38.395, p<0.001***	*F*(1,770) = 0.858, p=0.355
Alpha (8–13 Hz)	***F*(1,566) = 40.666, p<0.001***	***F*(1,566) = 26.350, p<0.001***